

PALOMAR/TRIPLESPEC OBSERVATIONS OF *SPITZER*/MIPSGAL 24 μm CIRCUMSTELLAR SHELLS:
UNVEILING THE NATURE OF THEIR CENTRAL SOURCES

N. FLAGEY^{1,4}, A. NORIEGA-CRESPO^{2,5}, A. PETRIC^{3,6}, AND T. R. GEBALLE⁶

Draft: July 23, 2018

ABSTRACT

We present near-IR spectroscopic observations of the central sources in 17 circumstellar shells from a sample of more than 400 “bubbles” discovered in the *Spitzer*/MIPSGAL 24 μm survey of the Galactic plane and in the Cygnus-X region. To identify the natures of these shells, we have obtained *J*, *H*, and *K* band spectra with a resolution ~ 2600 of the stars at their centers. We observed 14 MIPSGAL bubbles (MBs), WR149, and 2 objects in the Cygnus-X region (WR138a and BD+43 3710), our sample being about 2.5 magnitudes fainter in *K* band than previous studies of the central sources of MBs. We use spectroscopic diagnostics and spectral libraries of late and early type stars to constrain the natures of our targets. We find five late type giants. The equivalent widths of their CO 2.29 μm features allow us to determine the spectral types of the stars and hence derive extinction along the line of sight, distance, and physical size of the shells. We also find twelve early type stars, in nine MBs and the 3 comparison objects. We find that the subtype inferred from the near-IR for WR138a (WN9h) and WR149 (WN5h) agrees with that derived from optical observations. A careful analysis of the literature and the environment of BD+43 3710 allows us to rule out the carbon star interpretation previously suggested. Our near-IR spectrum suggests that it is a B5 supergiant. At the centers of the nine MBs, we find a WC5-6 star possibly of low-mass, a candidate O5-6 V star, a B0 supergiant, a B/A type giant, and five LBV candidates. We also report the detections of emission lines arising from at least two shells with typical extents ($\sim 10''$) in agreement with those in the mid-IR. We summarize the findings on the natures of the MBs since their discovery, with 30% of them now known. Most MBs with central sources detected in the near- to mid-IR have been identified and are red and blue giants, supergiants, or stars evolving toward these phases including, in particular, a handful of newly discovered Wolf-Rayet stars and a significant number of LBV candidates.

1. INTRODUCTION

Over 400 small ($\lesssim 1'$) rings, disks and shells have been discovered from visual inspection of the *Spitzer*/MIPSGAL 24 μm mosaic images (Carey et al. 2009; Mizuno et al. 2010). These MIPSGAL bubbles (MBs) are pervasive through the entire Galactic plane in the mid-infrared. They span a large range of morphologies, sizes and fluxes. All the MBs have also been observed with the IRAC instrument on board *Spitzer*, as part of the GLIMPSE survey (Benjamin et al. 2003). The GLIMPSE images indicate that only 10% of the MBs are detected between 3 and 8 μm . The analysis of the broadband images has also unveiled that 54 MBs (about 13%) have central sources at 24 μm . This number rises to at least 100 in the IRAC or 2MASS images (*J*, *H*, and *K* bands, Skrutskie et al. 2006). Several objects similar to the MBs have also been found in the Cygnus-X region, as reported

by Gvaramadze et al. (2010), Kraemer et al. (2010), and Gvaramadze & Menten (2012). Gvaramadze et al. (2010) and Wachter et al. (2010) reported the discovery of several tens of similar objects in addition to those of Mizuno et al. (2010) in the Galactic plane and the Cygnus-X region.

When Mizuno et al. (2010) published their catalog, only 15% of the MBs were identified or associated with stars of known spectral types. A large majority of the known MBs were found in the MASH Catalogue of planetary nebulae (PNe, Parker et al. 2006) and in the Catalogue of Galactic PNe (Kohoutek 2001). A few were associated with supernova remnants, Wolf-Rayet stars (WR), luminous blue variables (LBV) and other emission line stars. Most MBs were thus suspected to be associated with stars in late stages of evolution, with at least a fraction of them being massive. The extended mid-IR emission is expected to arise from warm, small dust grains and/or from hot ionized gas in the stellar winds and ejecta (Barniske et al. 2008), and it was confirmed by the *Spitzer*/IRS spectra later obtained for a small sample of MBs (Flagey et al. 2011; Nowak et al. in prep).

Optical and near-IR spectroscopic observations of the central sources in MBs discovered by *Spitzer* have successfully revealed several new WR and LBV candidates (Gvaramadze et al. 2010; Wachter et al. 2010, 2011; Stringfellow et al. 2012b). Most of these observations were performed on MBs with bright central sources detected at 24 μm . In this paper, we extend the identification of central stars in MBs to those fainter or not

nflagey@jpl.nasa.gov

¹ Jet Propulsion Laboratory, California Institute of Technology, 4800 Oak Grove Drive, Pasadena, CA 91109, USA

² Infrared Processing and Analysis Center, California Institute of Technology, 1200 East California Blvd, Pasadena, CA 91125, USA

³ California Institute of Technology, 1200 East California Blvd, Pasadena, CA 91125, USA

⁴ Institute for Astronomy, 640 North A'ohoku Place, Hilo, HI 96720-2700, USA

⁵ Space Telescope Science Institute, 3700 San Martin Dr, Baltimore, MD 21218, USA

⁶ Gemini North Observatory, 670 North A'ohoku Place, Hilo, HI 96720, USA

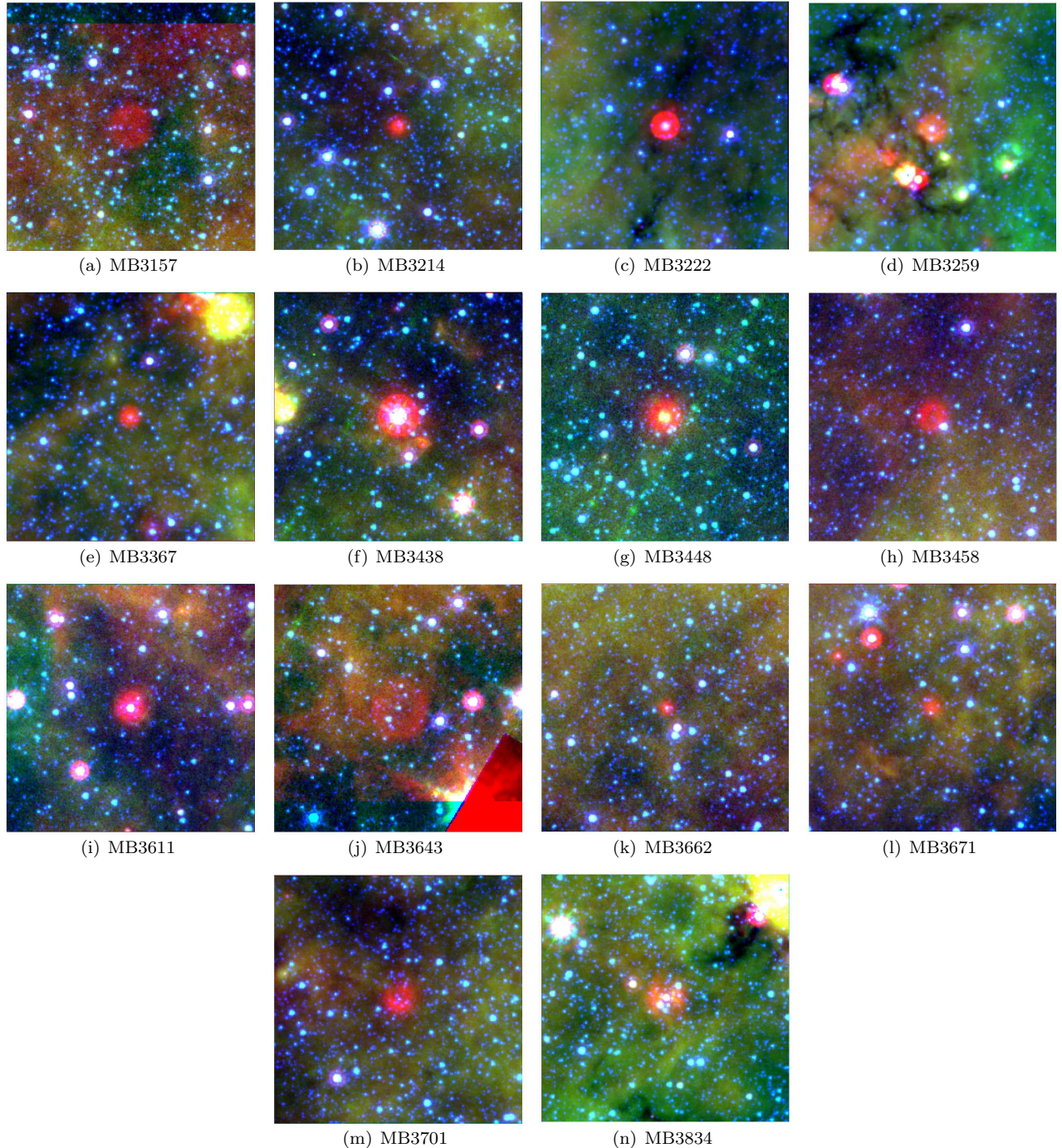


Figure 1. Three color images (red is MIPS24, green is IRAC8, blue is IRAC4 μm) of all the targets from Mizuno et al. (2010) in our sample. Each image is 5' by 5'. The color scale of each band differs in each image so to enhance the local structure.

detected in the MIPS GAL 24 μm images, using observations made at the Palomar Observatory with the near-IR Triple Spectrograph. Our sample comprises 14 MBs and 3 comparison sources.

The paper is organized as follows. In section 2 we detail the observations and data reduction. In section 3 we present our results, starting with the identification of the sources using the most prominent spectral features, and comparing our spectra to those in published libraries. We then characterize the few circumstellar shells that were detected in our spectroscopic observations. We summa-

rize the recent findings on the natures of the MBs collected over the past four years in section 4. Our conclusions are listed in section 5.

2. OBSERVATIONS

We acquired the data on August 21st and 22nd, 2010 at the Hale 200 inch telescope of the Palomar Mountain Observatory using the near-IR Triple Spectrograph (TripleSpec). TripleSpec uses a 1'' by 30'' slit and obtains a JHK , 1.0 to 2.4 μm , spectrum at a resolution of 2500-2700, with ~ 2.7 pixels per resolution element over a 1024x2048 pixel array. During our observations, the

Table 1
Summary of the observations

Target	Official nomenclature	2MASS source	Magnitudes			Classification
			<i>J</i>	<i>H</i>	<i>K</i>	
MB3157	MGE012.0365+01.0152	18081166-1801004	15.4	13.8	13.3	K0-K1 III
MB3214	MGE019.6490+00.7742	18240393-1126150	14.2	13.2	12.7	K2-K5 III ^{<i>j</i>}
MB3222	MGE030.1502+00.1239	18455526-0225089	17.7	14.2	11.7	Be/B[e]/LBV ^{<i>j</i>}
MB3259	MGE023.4497+00.0822	18334346-0823353	14.4	12.0	9.8	Be/B[e]/LBV
MB3367	MGE032.4980+00.1616	18500440-0018455	16.2	14.3	12.9	O5-6 V? ^{<i>i</i>}
MB3438	MGE042.0785+00.5085	19062457+0822015	9.7	7.9	6.9	Be/B[e]/LBV ^{<i>b, h</i>}
MB3448	MGE042.7663+00.8224	19063366+0907206	15.6	14.9	13.9	WC5-6 ^{<i>e</i>}
MB3458	MGE044.5868+00.7929	19100426+1043292	15.2	14.7	13.8	G8-K2 III
MB3611	MGE048.7813-00.8564	19240333+1339493	10.2	9.2	8.6	Be/B[e]/LBV ^{<i>c</i>}
MB3643	MGE042.9677-01.0182	19133273+0827030	12.4	11.0	10.5	K2-K5 III
MB3662	MGE038.7425-00.6984	19043348+0450567	13.2	12.2	11.7	B/A III
MB3671	MGE037.9741-00.7952	19032945+0407201	16.1	14.6	14.0	G4-G6 III
MB3701	MGE032.4004-00.1505	18510028-0032309	14.1	12.1	11.0	B0 I
MB3834	MGE019.8601-00.3578	18283340-1146441	14.4	11.4	9.7	Be/B[e]/LBV ^{<i>d</i>}
BD+43 3710		20453472+4332271	6.6	6.1	5.9	B5 I ^{<i>a</i>}
WR138a		20170811+4107270	10.2	9.3	8.6	WN9h ^{<i>f</i>}
WR149		21071169+4825361	10.6	10.1	9.6	WN5sh ^{<i>g</i>}

Note. — ^{*a*}BD+43 3710 was wrongly associated by Kraemer et al. (2010) with the nearby carbon star V2040 Cyg first discovered by Nassau & Blanco (1954), see section 3.2 for details. ^{*b, c, d*}These stars were identified as B[e]/LBV, Be, and B[e]/LBV respectively by Wachter et al. (2011). ^{*e*}This star was identified as a [WC] by Gvaramadze et al. (2010). ^{*f*}This star was identified as a WN8-9h by Gvaramadze et al. (2009). ^{*g*}This star was identified as a WN5s by Hamann et al. (2006). ^{*h*}This star was identified as a candidate LBV by Stringfellow et al. (2012b). ^{*i*}This nebula was suggested as a PN candidate by Ingallinera et al. (2014). ^{*j*}These nebulae are listed as PNe in SIMBAD, as suggested by Miszalski et al. (2008); Urquhart et al. (2009).

seeing was about 1'' or better.

The targets were chosen among the MBs that were unidentified at the time of the call for proposals, and that show at least one potential central source in the 2MASS or *Spitzer*/IRAC images (see Figure 1). For each of these MBs, we selected the star that appears as the best candidate for the actual central source. We also observed three comparison sources: the WN star WR149 (Hamann et al. 2006) and two objects in the Cygnus-X region that resemble some of the MBs: BD+43 3710 and WR138a, identified as a carbon star (Kraemer et al. 2010) and a WR star (Gvaramadze et al. 2009) respectively. Table 1 lists our targets and their near-IR magnitudes. The average *K* band magnitude of our sample (~ 11.5) was about 2 magnitudes deeper than the samples of Gvaramadze et al. (2010) and Wachter et al. (2010). Included also in Table 1 are the references for the MBs in our sample that have been identified since the time of our observations (MB3438, MB3448, MB3611, and MB3834). MB3214 and MB3222 are listed as PNe in SIMBAD. MB3214 is detected in H α and is listed as a True PN in the MASH-II catalog (Miszalski et al. 2008). MB3222 has been observed in the 6 cm radio survey of candidates massive young stellar objects by Urquhart et al. (2009) who suggested it is a PN.

The length of the slit allowed us to use the usual AB nodding observational strategy in most cases: the source was positioned about 5-10'' off center for a first exposure (A) before being moved to the opposite side of the slit for a second exposure (B). An immediate sky subtraction is thus performed while spending 100% of the time on-source. However, because our sources are in very crowded fields of the Galactic plane, we could not use this strategy for all the targets. In those cases, we spent only 50% of the time on-source and the remaining 50% were spent on a selected off-source position. Typical exposure times ranged from 20 to 300 seconds.

2.1. Data reduction

The data reduction was performed with XSpexTool v4.0beta for TripleSpec at Palomar developed by W. Vacca and M. Cushing (Cushing et al. 2004; Vacca et al. 2004). This IDL widget package extracts the spectrum from each exposure, taking into account the wavelength calibration performed on the atmospheric lines, the bias and the flat field corrections, and then combines all the exposures together. We did not use XSpexTool to remove the telluric absorption and calibrate the spectra because it assumes the standards are of A0 V type while we observed F and G type stars. Instead we used our own routine and F and G star spectral templates from the IRTF Spectral Library (Rayner et al. 2009). For each target we tried several standards for which the airmass and the time of observation were close to those of the source of interest and chose the final spectrum that shows the best overall quality in terms of signal-to-noise ratio and low atmospheric line residuals. The resulting spectra are shown in Figures 2, 3, 4, and 5, after normalization by a polynomial fit to the continua.

3. RESULTS

The 17 targets in this program can roughly be separated into two groups: eight stars with near-IR spectra dominated by absorption lines and nine stars whose spectra show many emission lines. For each of these two groups, two sub-groups can be defined. In the ‘‘absorption’’-dominated group, five targets exhibit the CO band-head absorption features at 2.29 μm and beyond, characteristic of G and later type giants and supergiants, while three stars show hydrogen and helium transitions in absorption, more typical of B and A type stars. In the ‘‘emission’’-dominated group, four sources exhibit the He II 2.189 μm line characteristic of O and WR stars, while the five other targets are set apart by the absence of the He II line and the presence of metal lines

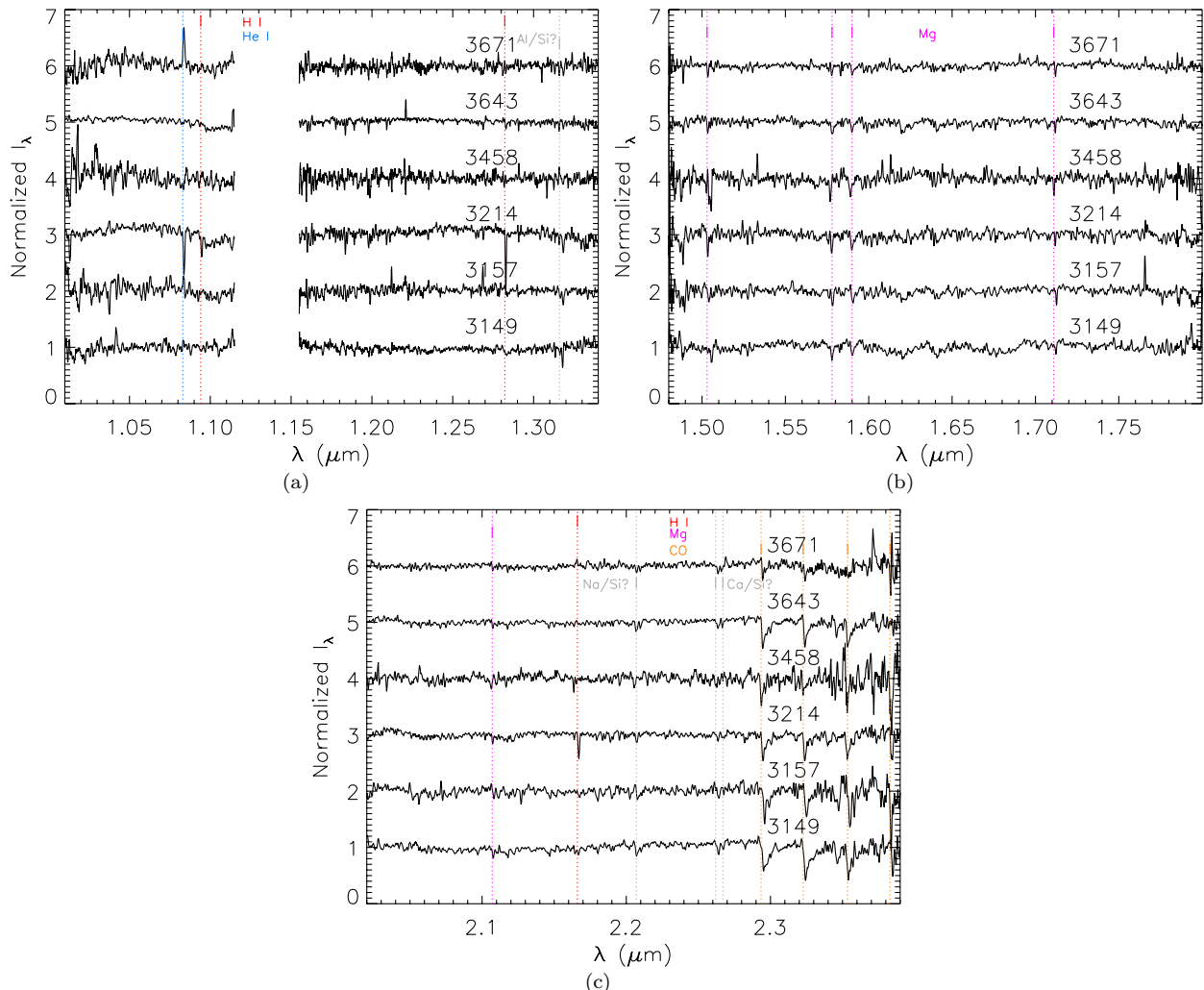


Figure 2. Near-IR spectra (a: J band, b: H band, c: K band) of the late type stars in our program. The most prominent lines are indicated by vertical dashed lines of different color for different species.

in emission, which are more common in LBV candidates. We discuss each sub-group separately. We close this section with the unexpected detection of several shells in our observations.

3.1. Late type stars: G and K giants

The near-IR spectra of the five stars that exhibit CO band-head absorption features are shown in Figure 2. The K band is dominated by the $\Delta v = 2$ band-head features at $2.29 \mu\text{m}$ and beyond. Several other absorption lines due to metals can be found (e.g. Mg at 1.58 and $1.59 \mu\text{m}$, Si or Al at $1.31 \mu\text{m}$, Si or Na at $2.2 \mu\text{m}$, Si or Ca at $2.26 \mu\text{m}$) although they are significantly weaker and their identification thus remains difficult.

Figer et al. (2006) and Davies et al. (2007) have shown that there is an anticorrelation between E_{CO} , the equivalent width of the $2.29 \mu\text{m}$ feature, and the star’s temperature. We measure E_{CO} the same way it was done by Figer et al. (2006) and Davies et al. (2007). The two estimates of the equivalent width are reported in Table 2 for the five late-type stars in our sample. The classifications then inferred from the work of Figer et al. (2006) and Davies et al. (2007) usually agree within a few subtypes at most. Assuming the near-IR colors and absolute

magnitudes for red giants and supergiants from Allen’s Astrophysical Quantities (Cox 2000), assuming the interstellar extinction curve from Cardelli et al. (1989), and using the 2MASS J and K band magnitudes, we derive the visual extinction towards each source and its distance. We rule out the supergiant interpretation for each of them, based on the average extinction along the line of sight. On average, we expect about 2 mag/kpc of visual extinction using $A_V/N_H = 0.53 \times 10^{-21} \text{ cm}^2$ and an average interstellar gas density of 1 cm^{-3} along the line of sight (also see Whittet 2003). In the supergiant scenario, the five sources would be along lines of sight with at most 0.2 mag/kpc . The derived distances also rule out the supergiant interpretations for all targets, under the hypothesis that these are Galactic objects. In the supergiant scenario, the five sources would instead be located between 36 and 183 kpc from the Sun and have sizes in the range $8\text{--}22 \text{ pc}$.

For the preferred giant interpretation, we derive the size of the $24 \mu\text{m}$ shell for each late-type star. We find that the five shells are between 0.7 and 1.3 pc in radius. These sizes are larger by at least a factor of two than those derived by Young et al. (1993) from IRAS $60 \mu\text{m}$ observations of red giant stars and young PNe (less than

Table 2Equivalent width of the CO 2.29 μm band-head features and inferred spectral type, extinction, distance, and shell size.

Target	E_{CO} (\AA)	Spectral type	A_V	d (kpc)	24 μm radius	24 μm size (pc)
MB3157	10.1 ^a / 16.8 ^b	G6-G7 I ^a / G8-G9 I ^b	9.0 \pm 0.1	120 \pm 3	35''	20
		K0-K1 III^a / K0-K1 III^b	8.3\pm0.1	6.8\pm0.5		1.2
MB3214	11.9 ^a / 24.8 ^b	G7-G8 I ^a / K0-K1 I ^b	5.4 \pm 0.3	112 \pm 5	20''	10
		K2-K3 III^a / K4-K5 III^b	3.7\pm0.1	11.8\pm4.1		1.1
MB3458	7.2 ^a / 19.3 ^b	G4-G5 I ^a / G9-K0 I ^b	5.0 \pm 0.3	183 \pm 10	25''	22
		G8-G9 III^a / K1-K2 III^b	4.3\pm0.4	10.4\pm2.1		1.3
MB3643	14.3 ^a / 21.3 ^b	G9-K0 I ^a / G9-K0 I ^b	7.7 \pm 0.1	36.3 \pm 0.5	45''	7.7
		K4-K5 III^a / K2-K3 III^b	6.5\pm1.1	3.4\pm1.8		0.7
MB3671	4.7 ^a / 6.9 ^b	G2-G3 I ^a / G6-G7 I ^b	9.3 \pm 0.2	157 \pm 7	20''	15
		G5-G6 III^a / G4-G5 III^b	8.8\pm0.1	7.1\pm0.3		0.7

Note. — ^a values derived using the method of Davies et al. (2007), ^b values inferred using the method of Figer et al. (2006). For each of the 5 late type stars, the first line gives the parameters for a supergiant while the second line gives those for a giant. In **bold** is our suggested identification.

0.3 pc mostly). This difference might be due to a distance selection effect, because IRAS could only resolve nearby ($\lesssim 1$ kpc) objects. They are smaller than the sizes found by Stencel et al. (1989) in their analysis of supergiant stars (between 1 and 3 pc), which also used IRAS 60 μm observations. Wachter et al. (2010) found 12 late-type stars in their sample of objects similar to ours, and suggested that all but one are supergiants. The shell sizes they derived range from 0.4 pc for the only suggested giant, to 0.5-3 pc for the supergiants. These sizes are consistent with the sizes we inferred for our sample.

3.2. Early type stars: B and A stars

Three targets in our sample have spectra dominated by hydrogen and/or helium transitions in absorption, which are characteristics of early type (B and A) stars. These targets are BD+43 3710, MB3662, and MB3701 (see Figure 3).

BD+43 3710 - This source has been associated with a carbon star of spectral type R: by Kraemer et al. (2010) based on the initial discovery by Nassau & Blanco (1954). However, the table where the actual carbon star was found in the latter paper “gives a reference BD star near the carbon star”, implying that the carbon star is not BD+43 3710. Nassau & Blanco (1954) wrote that the carbon star was found 0.6 mm to the East and 1.2 mm to the South of the BD star, “in the scale of the BD chart from the reference star to the carbon star”. The plate scale of the Bonner Durchmusterung is 3' per mm, which locates the carbon star about 1.8' to the East and 3.6' to the South of BD+43 3710. In the 2MASS *JHK* images near BD+43 3710, a bright and red star ($J=5.55$, $H=4.046$, and $K=3.26$) is visible at about 1.8' to the East and 3.2' to the South. This star is 2MASS 20454509+4329181, also known as V2040 Cyg, and is referenced as a semi-regular pulsating carbon star in SIMBAD (Aaronson et al. 1990). A spectral type N5 was found for V2040 Cyg by Eglitis et al. (2003). Its R and J magnitudes of 10.8 and 6.6, respectively, seem like a good match to the infrared magnitude m_i of about 9 reported by Nassau & Blanco (1954). We therefore suggest that the carbon star of Nassau & Blanco (1954) is V2040 Cyg.

The near-IR spectrum of a carbon star usually shows broad, molecular features of CN and C₂ over the entire near-IR range, as well as the CO band-head absorption features at 2.29 μm and beyond (e.g. Rayner et al.

2009). The near-IR spectrum of BD+43 3710 however shows strong absorption in the hydrogen transitions of the Brackett and Paschen series, and in the He I transitions. The strength of the H absorption lines, combined with the detection of He I lines in absorption indicates a good match to B type stars (see e.g. Lancon & Rocca-Volmerange 1992; Hanson et al. 2005). The best match is the B5 supergiant HR2827 (Meyer et al. 1998). We favor this luminosity class because of the narrow absorption lines. Giants and dwarfs usually have significantly broader absorption features than supergiants, because of their higher gravity.

To test the validity of our interpretation of BD+43 3710, we use the intrinsic colors for early supergiants (Allen 1983) and estimate its distance and the extinction along the line of sight. We use the B and V magnitudes referenced in SIMBAD, as the near-IR magnitudes may be contaminated by hot dust emission. Assuming a B5 I spectral classification, we find that BD+43 3710 is at about 2.5 kpc, just behind the Cygnus-X region, and that the total visual extinction along the line of sight is 3 mag. At 2.5 kpc, the 2.7' by 0.9' mid-IR shell of BD+43 3710 would have a physical size of 2.0 by 0.7 pc.

MB3701 and MB3662 - The spectra of the stars at the centers of these MBs are slightly different from that of BD+43 3710. The former shows weaker absorption in the hydrogen transitions but stronger in He I, while the latter shows stronger hydrogen but weaker He I absorption lines. This suggests an earlier type for the star at the center of MB3701 than for BD+43 3710, and a later type for that in MB3662. As for the BD star, we favor the supergiant luminosity class based on the width of the absorption features for the central star of MB3701, although the limited number of these features prevents us from reaching a clear conclusion. For example, the spectrum of HR1903 (B0 I, Meyer et al. 1998; Wallace et al. 2000) is a good match to that of the central source in MB3701. For the star in MB3662, the widths of the hydrogen lines in H band are slightly larger than those of the BD star, which could suggest a higher luminosity class. In terms of the absorption features relative intensities, the spectra of HR3975 and HR2827 (A0 I and B5 I respectively, Meyer et al. 1998) are both good matches to that of the central star in MB3662, especially because the He line at 1.7 μm is still present. However, HR1552 and HR5291 (B2 III and A0 III respectively) seem to be

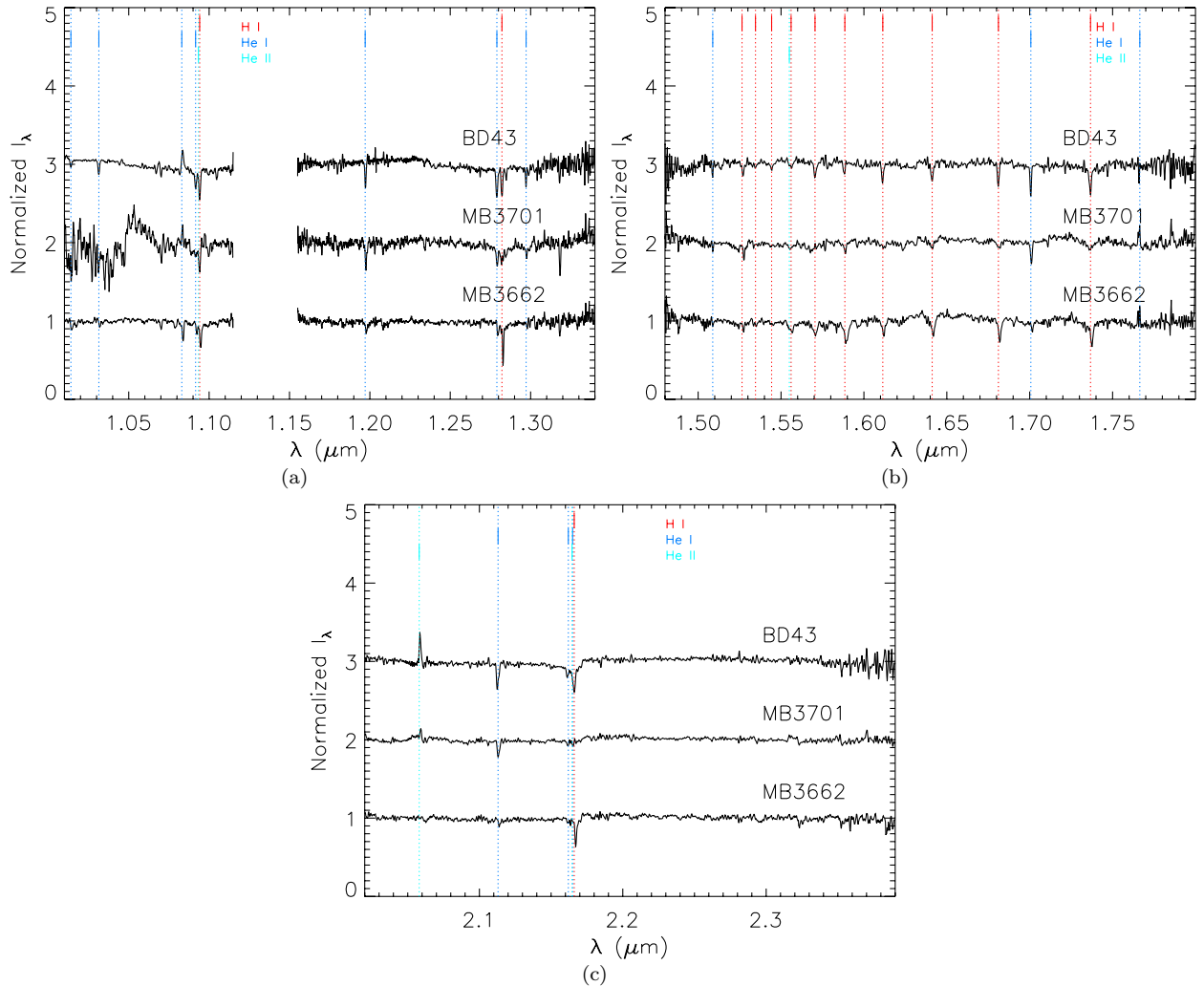


Figure 3. Near-IR spectra (a: *J* band, b: *H* band, c: *K* band) of the OBA type stars in our program. The most prominent lines are indicated by vertical dashed lines of different color for different species.

better suited in terms of line widths.

Unlike BD+43 3710, the star at the center of MB3662 is faint in the optical ($B \sim 21$ mag, $V = 18.6$ mag). Assuming $A_B/A_R = 1.79$, we find that as an A0 or B5 supergiant, this source would be too far away ($\gtrsim 16$ kpc) and with too little extinction along the line of sight ($A_V \sim 8$ mag). We therefore favor a higher luminosity class (e.g. B5 III) for this star. We use the intrinsic colors published by Pickles (1998) and find that MB3662 would then be at 3.7 kpc with about 8.3 mag of extinction along the line of sight. At that distance, MB3662 would be about 0.3 pc in radius. For the star at the center of MB3701, only near-IR magnitudes are available. We infer from them that MB3701 would be at about 14 kpc with a visual extinction of about 15 mag, assuming a B0 I spectral classification. The average extinction towards MB3701 would be in fair agreement with the average Galactic value, and the physical radius of MB3701 would be about 1.7 pc. However, an IR excess can contribute to the central source fluxes and a slightly different spectral type or luminosity class remains possible for MB3701.

3.3. Emission line stars

Among the nine spectra that are dominated by emission lines, four exhibit many unresolved emission lines while the five others are dominated by broad lines. Broad lines are an indication of strong stellar winds, which can be found in WR stars, where typical velocities are above 1000 km/s (Crowther 2007). LBV stars are also known for their stellar winds with velocities of a few 100 km/s. Instead of using the presence of broad lines, we use the presence of the He II lines at 1.012 and 2.189 μm as a strong indication that a given source is an O or WR star, following the studies of Morris et al. (1996), Figer et al. (1997), Crowther et al. (2006), and Wachter et al. (2010).

Four targets (MB3448, MB3367, WR149, and WR138a) show either or both of the He II lines in their spectra (see Table 3). WR149 and WR138a are both known WR stars with mid and late WN type respectively. The five sources that do not show the He II lines (MB3222, MB3259, MB3438, MB3611, and MB3834) have also in common that their spectra exhibit many emission lines of metal species: Fe lines at e.g. 2.09 and 1.69 μm , the Mg doublet at 2.138-2.144 μm , and the Na doublet at 2.206-2.209 μm . Such lines have been observed preferentially, but not exclusively, in LBV,

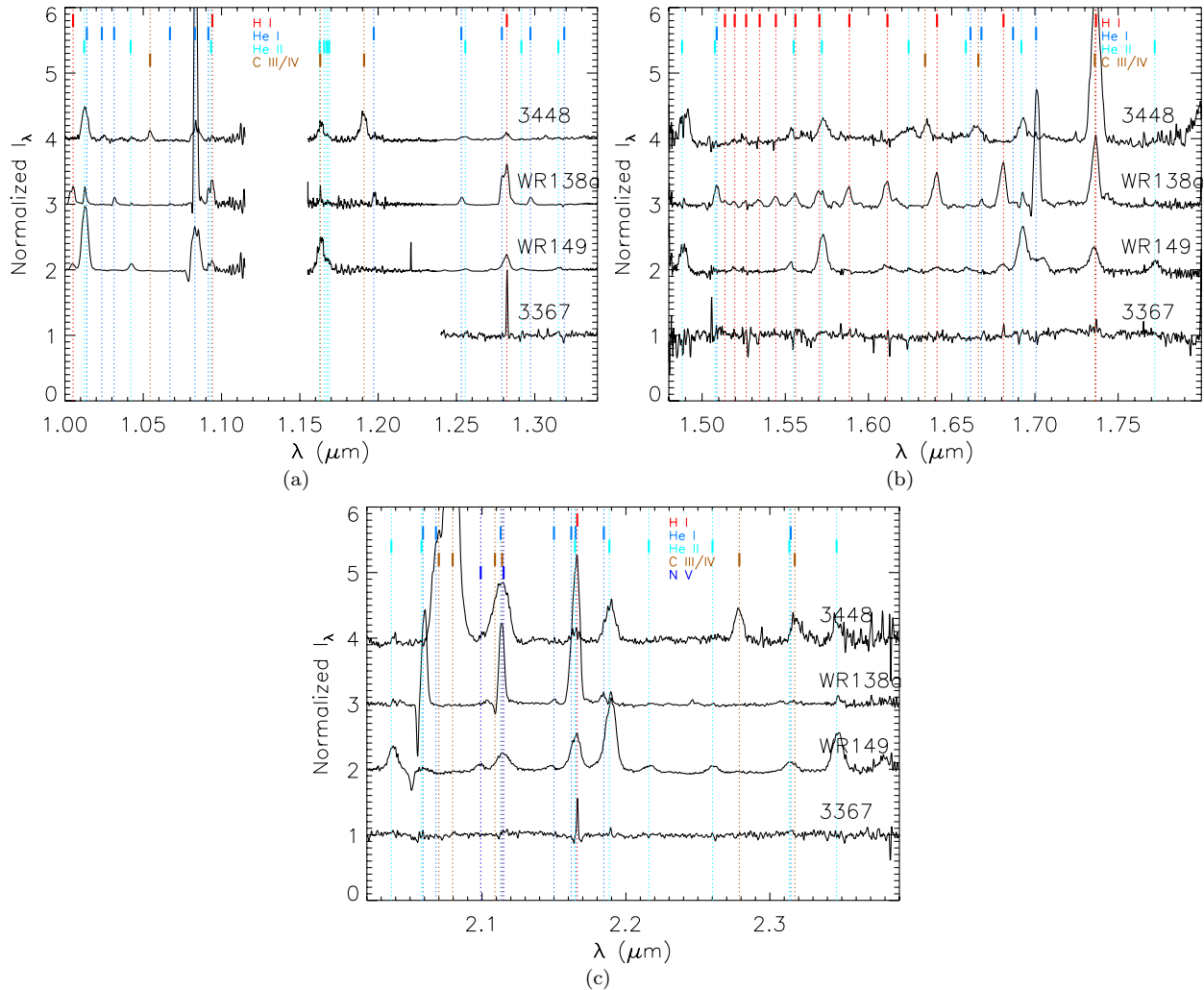


Figure 4. Near-IR spectra (a: *J* band, b: *H* band, c: *K* band) of the emission line stars that we suggest as O and WR candidates. For the star at the center of MB3367, the short wavelengths end of the *J* band spectra are mostly useless and therefore not shown. The most prominent lines are indicated by vertical dashed lines of different color for different species.

B[e], and Be stars (e.g. Morris et al. 1996). MB3438, MB3611, and MB3834 have been suggested as B[e]/LBV, Be, and B[e]/LBV, respectively by Wachter et al. (2011), and Stringfellow et al. (2012b). A clear distinction thus seems to emerge between O and WR and LBV candidates, based on the presence of the He II lines at 1.012 or 2.189 μm , or the presence of emission lines of Fe, Mg or Na.

3.3.1. *O* and *Wolf-Rayet* stars

The spectra of the four O and WR stars are shown in Figure 4. The four spectra are quite different from each other. We use the classification diagnostics of Crowther et al. (2006), based on line equivalent width ratios, to derive the subtype of each WR star. The equivalent widths of the diagnostic lines are indicated in Table 4.

WR149 - WR149 is a WN5-s star, where the “s” indicates strong lines (Hamann et al. 2006, based on optical observations). The near-IR spectrum of WR149 shows strong helium lines with P Cygni profiles, and strong hydrogen lines. Several N lines, including the N V line at 2.099 μm , which is a clear indicator of early type WN stars, are also detected. The three near-IR diagnostics

of Crowther et al. (2006) for WN stars indicate a WN5-6 subtype, in very good agreement with that inferred from the optical observations. Due to the presence of hydrogen lines in emission, we suggest that this star be identified as WN5h. The P Cygni profiles of the He I lines allow us to estimate the speed of the wind in WR149, using a method similar to that presented by Voors et al. (2000). We find a terminal velocity of about 1700 km/s, in good agreement with the 1300 km/s found by Hamann et al. (2006) and with the typical velocities in WN5 stars (1500 km/s, Crowther 2007).

WR138a - This source is a WN8-9h star (Gvaramadze et al. 2009, based on optical observations). The near-IR spectrum of WR138a exhibits strong helium lines with P Cygni profiles, and strong hydrogen lines. However, unlike that of WR149, it does not show nitrogen lines, although the N III 2.115 μm line could be blended with the He I line at 2.11 μm . The diagnostics of Crowther et al. (2006) indicate a WN9 subtype. A WN8 subtype would have significantly larger He II 1.012 μm to He I 1.083 μm , and He II 2.189 μm to Br γ equivalent width ratios. We suggest that this star be identified as a WN9h to take into

Table 3
Line detection used for the identification of the early type stars

Target	He II 1.012 μm	He II 2.189 μm	Mg II 2.138/2.144 μm	Na II 2.206/2.209 μm	Fe II 1.69/2.09 μm	C III/C IV 1.20/2.08 μm
MB3222			✓			
MB3259			✓	?	✓	
MB3438			✓	✓	✓	
MB3611			✓	✓	✓	
MB3834			✓	?	?	
MB3367	?	✓				
MB3448	✓	✓				✓
WR138a	✓	✓				
WR149	✓	✓				

Note. — A ✓ indicates a clear detection while a ? indicates a questionable detection.

Table 4
Line equivalent widths used for the determination of the Wolf-Rayet stars subtypes

Target	He II 1.012 μm	He I 1.083 μm	He II 2.189 μm	Br γ	N V 2.099 μm	N III/He I 2.115 μm	C IV 1.191 μm	C III 1.198 μm	C IV 2.076 μm	C III 2.110 μm
MB3367		70	0.9	5						
MB3448							140	20	410	170
WR138a	13	380	3	94						
WR149	170	188	68	33	6	23				

Note. — Units are angstroms.

account the emission lines of hydrogen. The P Cygni profiles of the He I lines allow us to estimate the speed of the stellar wind in WR138a, using the same method as for WR149. We find a velocity of about 650 km/s, in excellent agreement with the 700 km/s found by Gvaramadze et al. (2009) and with the typical velocities in WN9 stars (700 km/s, Crowther 2007).

MB3448 - The spectrum of the star at the center of MB3448 is dominated by strong C emission lines with FWHMs of about 1000-1500 km/s, which are characteristic of late type WC stars (1200 km/s for WC9, 1700 km/s for WC8, Crowther 2007). The classification diagnostics of Crowther et al. (2006) for WC stars indicate either a WC5-6 or a WC8 subtype. Because the lines are broad, features are blended and the uncertainties in some equivalent widths may be large. The typical wind velocities for WC5-6 stars (2200 km/s, Crowther 2007) are significantly larger than those we measure but the C IV 1.191 to C III 1.198 μm line ratio clearly suggests an earlier type than WC8. We thus favor a narrow-line WC5-6 interpretation. Using intrinsic colors and magnitudes for WC5-6 stars in the optical from van der Hucht (2001) and Crowther (2007), assuming $m_V \sim 18.6$ mag for the star at the center of MB3448 ($B = 19.9$ and $R = 17.4$), and that $A_B = 1.31 \times A_V$, we find that MB3448 would be at a distance of about 25 kpc and suffer only about 5 mag of visual extinction. At that distance, MB3448 would be about 1.5 pc in radius. We note however that the intrinsic magnitude of WC6 stars could be significantly lower ($M_v \sim -4.3$ in Sander et al. 2012) and the distance even larger. Kanarek et al. (2014) recently listed this star as a WC6, with an uncertainty of up to two subtypes. Assuming it is a massive WR star, they derive a distance of almost 30 kpc, in good agreement with our estimates. However, the average extinction along the line of sight would be significantly smaller than that expected in the interstellar medium. Gvaramadze et al. (2010) identified the star at the center of MB3448 as a

[WC] but did not show a spectrum. They favor the low-mass WR interpretation because MB3448 has an optical counterpart, which suggests a distance significantly smaller than those derived in the high-mass WR case. There are no tabulated values for the intrinsic colors of [WR] stars. Parker & Morgan (2003) found M_V between -1 and 0 for a few [WC] stars. Leuenhagen et al. (1996) gave parameters for five [WC] stars, from which values of M_V between -2.7 and +1 are derived. Assuming the colors of a [WC5-6] are the same as those of a WC5-6, and $M_V \sim -0.5$, MB3448 would be at a distance of ~ 6 kpc. The shell would then be about 0.5 pc in radius.

MB3367 - The spectrum of the central source in MB3367 is dominated by a few, unresolved emission lines (Pa β , Br γ , He II line at 2.189 μm) and several absorption features (e.g. Br γ , He I at 1.70 μm). Possible emission is detected at 2.11-2.12 μm (He I or N V). The overall signal-to-noise ratio of the spectrum is among the lowest of our sample, due in part to large variations of airmass during the observations. The He II 2.189 μm to Br γ equivalent width ratio indicates a WN8 subtype (Crowther et al. 2006), but one would expect a strong stellar wind (~ 1000 km/s, Crowther 2007) while the lines are unresolved in our spectra (≤ 130 km/s). The shape of the spectrum around Br γ evokes that of an O star with nebular emission. Furness et al. (2010) obtained H and K -band spectra of O stars in W31: their #5 in particular, an O5-6 V star, is a very good match to the central star in MB3367. Using near-IR colors for O5 dwarfs (Allen 1983), we find that MB3367 is behind ~ 23 mag of visual extinction and at a distance of about 11 kpc. As a supergiant, it would be at about 16 kpc, although the apparent widths of the absorption features in the spectrum suggest a lower luminosity class. At a distance of 11 kpc, MB3367 would have a radius of about 0.5 pc. Ingallinera et al. (2014) suggested that MB3367 is a PN candidate based on 6 and 20 cm observations, but could not entirely rule out the thermal emission hypothesis.

While we favor the O5-6 V nature for the star at the center of MB3367, we cannot completely rule out other interpretations.

3.3.2. LBV candidates

The spectra of the five LBV candidates are shown in Figure 5. In addition to the metal lines listed in Table 3, the spectra also show H and He I emission lines. Variations, both subtle and significant, especially in terms of the intensities and widths of the H and He I lines, are found in this group, as Wachter et al. (2010) observed in their group of Be/B[e]/LBV candidates.

MB3438 - The spectrum of the central source shows strong hydrogen lines, including the Pfund series at wavelengths longer than 2.3 μm and the Brackett series down to about 1.5 μm , and many metal lines. Helium lines are weak or in absorption (e.g. 1.70, and 2.11 μm). The overall spectrum is nearly identical to those of Be/B[e]/LBV in the Group 2A of Wachter et al. (2010). Wachter et al. (2011) classified it as a B[e]/LBV star, although no reason was given to rule out the Be interpretation.

MB3259 - The spectrum of the central source in MB3259 is similar to that of the star at the center of MB3438, except that most H lines are significantly weaker, especially in the *H* band, although iron lines are relatively stronger.

MB3611 - The spectrum of the central source in MB3611 is similar to that of the star at the center of MB3438, although no iron lines are detected except perhaps in the *J* band at 1.05, 1.09, and 1.25 μm . On the contrary, many H lines are detected in the Brackett series and possibly in the Pfund series. Multiple He I transitions are seen in absorption in the *J* band. Wachter et al. (2011) classified it as a Be star. However, their motivation for such classification was not given.

MB3222 - The star at the center of MB3222 is very faint in the *J* band (17.7 mag) and the spectrum we have obtained has an insufficient signal-to-noise ratio to be shown here. The *H* band spectrum also suffers from significant residual emission due to the telluric lines and only part of it is shown in Figure 5. Compared to the spectrum of the central source in MB3438, that of the star at the center of MB3222 shows no iron lines. The He I lines in emission (e.g. at 2.112, 1.7 μm) exhibit P Cygni profiles. We follow the same method as for WR149 and infer a terminal velocity of the wind in MB3222 of about 200 km/s, which is in agreement with an LBV nature.

MB3834 - The spectrum of the star at the center of MB3834 shows broad and strong H lines in the Brackett series down to below 1.55 μm and strong He I lines in emission with P Cygni profiles. Iron lines may be detected at 1.64, 1.68, or 1.69 μm , but each may be blended with H or He I lines. The most plausible detections of iron lines are at 1.74 μm and around 1.62 μm . Using the same method as for WR149, we infer a terminal velocity of the wind in MB3834 of about 550 km/s, which is in agreement with an LBV nature. Wachter et al. (2011) classified it as a B[e]/LBV star, although no reason was given to rule out the Be interpretation.

In summary of section 3.3, we confirm in the near-IR the spectral types of WR149 and WR138a and

three LBV candidates, previously obtained in the optical domain and, among the MBs, identify a WC5-6 star possibly of low mass, a candidate O5-6 star possibly dwarf, and two Be/B[e]/LBV candidates. As pointed out by Morris et al. (1996) and Wachter et al. (2010), the *JHK* spectra of Be, B[e], and LBV stars are almost identical, although the natures of the objects are quite different. Detailed discussions about Be stars can be found in Jaschek et al. (1981), Collins (1987), and Porter & Rivinius (2003), about the B[e] phenomenon in Lamers et al. (1998) and Bjorkman et al. (1998), and about LBVs in Humphreys & Davidson (1994), Nota et al. (1995) and Clark et al. (2005). Lenorzer et al. (2002) has established a diagnostic, based on hydrogen lines in the *L* band, to distinguish between Be stars, B[e] phenomena, and LBVs. Spectroscopic observations in the 3-4 μm range of the many LBV candidates among the central sources of MBs could thus remove the ambiguity inherent to their *JHK* spectra.

3.4. Detections of near-IR shells

While the main goal of our observations is to identify the spectral types of the stars at the centers of the MBs, we also report for the first time the discovery of several shells in the near-IR spectroscopic observations. They appear very clearly in the differences between the two nodding positions. The MBs with detected shells are MB3214, MB3367, and MB3438. However, in MB3438, the compact extended emission is difficult to assess due to the intensity of the central point source. The lines for which we claim a clear detection of extended emission are the Pa δ 1.006, He II 1.012, He I 1.083, Pa γ 1.095, He II 1.163, Pa β 1.283, Br(11-4) 1.682, Br(10-4) 1.737, He I 2.060, Br γ 2.168, and He II 2.189 μm . These lines are all detected in MB3214 while only some are in MB3367.

To measure the spatial and velocity extent of a detected shell, we first “rectified” the 2D image from TripleSpec using an IDL code written by P. Muirhead and J. Wright⁷. All the orders of the spectrograph are concatenated and their curvatures corrected so the data appear as a long 2D array, where one dimension indicates the wavelength while the other indicates the position along the slit. We do this on the difference between the two nodding positions, which allows us to subtract the continua from the stars in the slit (by removing the median value along each spatial column of pixels), and the atmospheric lines (by removing the median value along each spectral row of pixels), and thereby to produce position-wavelength and position-velocity diagrams of the shells. Figure 6 shows such diagrams for the He I 1.083 μm , Pa β , and Br γ lines in MB3214 and MB3367. Both nodding positions are visible, each on one side of the slit. We note a slight but systematic shift in the wavelength position of the lines towards both targets. For MB3214, the shift is about 250 km/s while it is about 100 km/s for MB3367. Part of this shift could be due to wavelength calibration errors. However, the fact that the shift is systematic indicates that it is real. Using a Galactic rotation curve with $V_{sun} = 254$ km/s and $R_{sun} = 8.4$ kpc (Reid et al. 2009), we find that toward MB3214 ($l \sim 20^\circ$), v_{LSR} could reach values higher than

⁷ http://astrosun2.astro.cornell.edu/~muirhead/tspec_rectify.pro

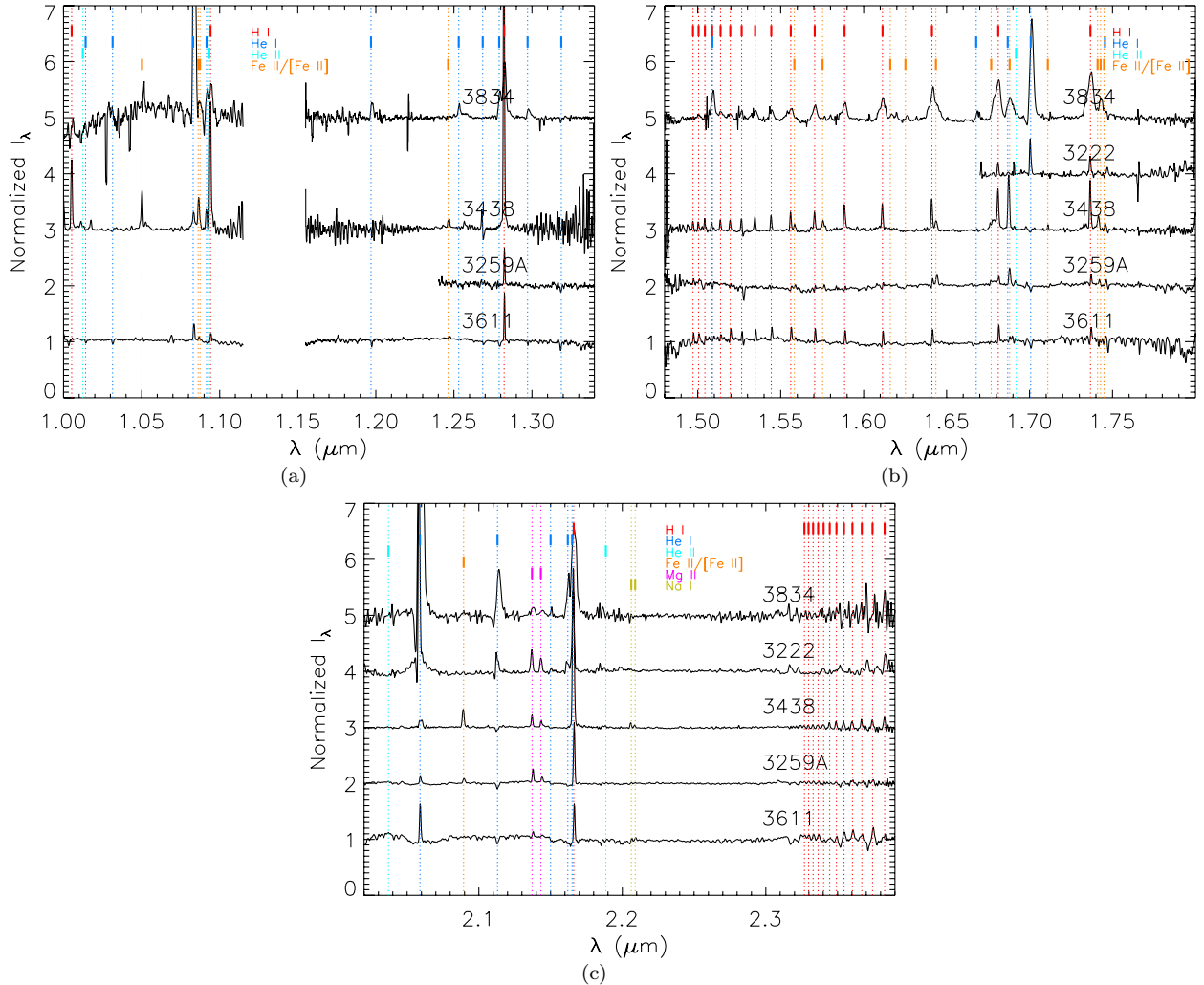


Figure 5. Near-IR spectra (a: *J* band, b: *H* band, c: *K* band) of the emission line stars that we suggest as LBV candidates. For the stars at the center of MB3222 and MB3259, the short wavelengths end of the spectra are mostly useless and therefore not shown. The most prominent lines are indicated by vertical dashed lines of different color for different species.

150 km/s between 7 and 9 kpc from the Sun, which is in agreement with our estimates based on the spectral type of the star in MB3214 (11.8 ± 4.1 kpc, see section 3.1). Toward MB3367 ($l \sim 32^\circ$), v_{LSR} reaches 100 km/s or above between 5 and 10 kpc from the Sun, in fair agreement with the 11 kpc we suggest if MB3367 has an O5-6 V star at its center (see section 3.3.1). However, because the MBs appear to be isolated, chances are they are runaway stars (e.g. Gvaramadze et al. 2012): their radial velocities could thus be significantly different from the average motion of the Galaxy in their vicinity.

From the position-velocity diagrams, we also infer that the shells are barely resolved. Toward MB3214, we measure a $\lambda/FWHM$ of 2400, 2200, and 2400 at $\lambda = 1.083$, 1.283, and 2.168 μm respectively, which correspond to about 130 km/s. Toward MB3367, those values are 2200, 2400, and 2600 respectively. These values are very close to the resolution of TripleSpec. We therefore cannot rule out that there is some intrinsic broadening of the lines. Along the spatial dimension, we first note that the shell of MB3214 shows a “lobe” on each side of the central star, extending out to about $9''$ with a “hole” of about $1-2''$ radius near the source. The shell of MB3367 shows

a single structure that extends about $5''$ from the central source. In the MIPS24 μm images, neither object shows a central “hole”, and we measure a radius of 10-15'' for MB3214 and of 7-11'' for MB3367. However, the angular resolution of the MIPS24 μm images is $6''$. Therefore, the radius of the shell measured in the near-IR seems in good agreement with that derived from the mid-IR images. The emission lines observed in the near-IR thus arise from the same region that dominates the mid-IR emission. Flagey et al. (2011) and Nowak et al. (in prep) have shown that they can be accounted for by highly ionized gas emission, warm dust, or a mix of both.

4. SUMMARY OF THE FINDINGS ON THE MBS

When Mizuno et al. (2010) published their catalog, about 85% of the MBs were completely “unknown” (i.e. they had never been detected in previous observations or no spectral type had been suggested for their central star, if any has been detected). Among the “known” MBs, about 80% were identified as PNe while the others comprised supernova remnants, luminous blue variables and other emission line stars. The PNe especially dominated the group of MBs for which no central star was detected at 24 μm . About four years later, combining the

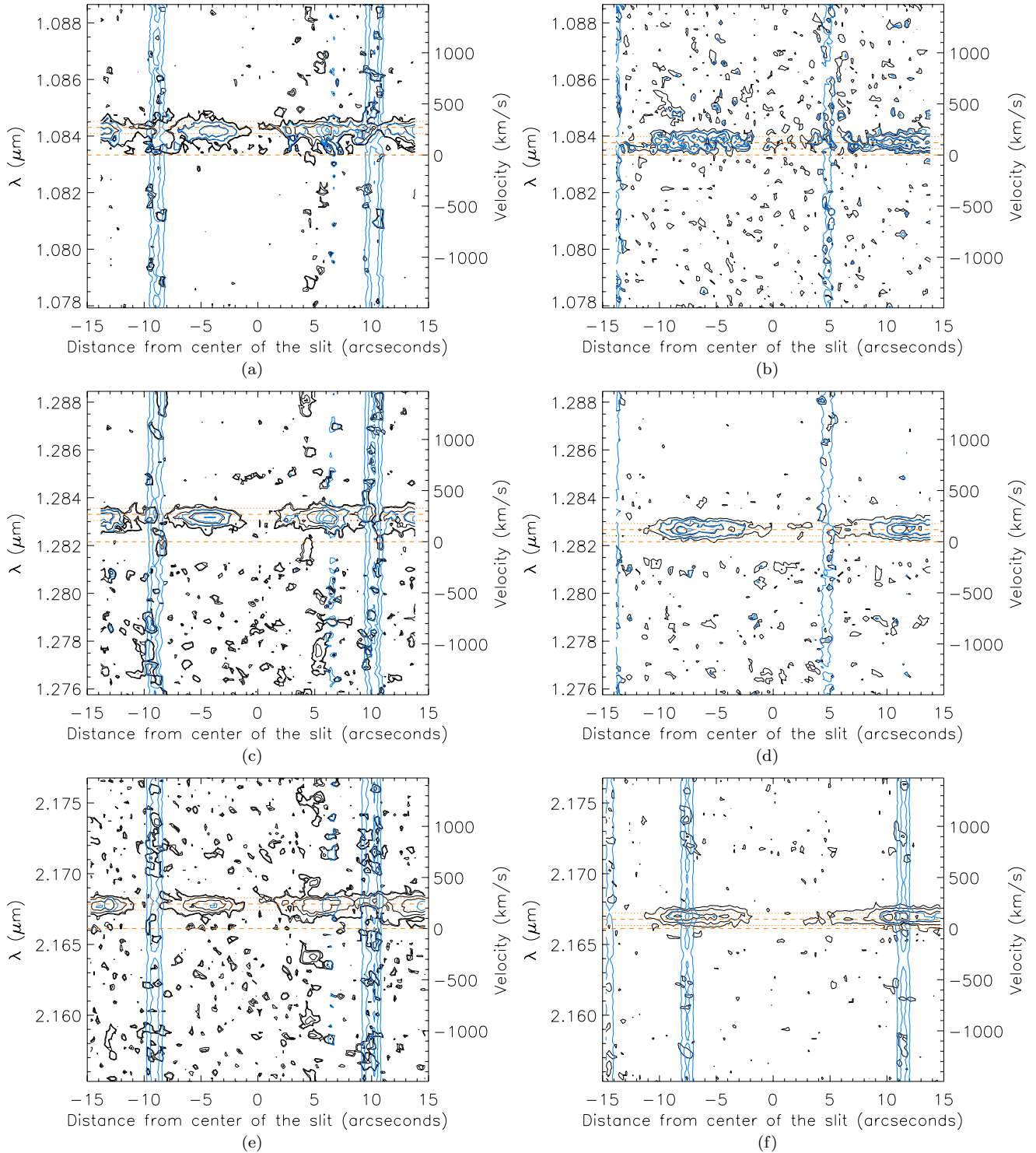


Figure 6. Position-lambda or position-velocity diagrams for the He I 1.083 μm , Pa β , and Br γ lines (*from top to bottom*) towards MB3214 (*left*) and MB3367 (*right*). In each panel, NodA is on the right of the slit while NodB is on the left. Contours are at 7.5, 10, 25, and 50% of the peak intensity in the spectral and spatial range shown, after background (star and atmosphere) subtraction for MB3214, and 10, 25, 50 and 75% for MB3367. Contours in blue are inferred the same way but before subtraction of the star contribution to highlight the position of the central source, at about $-10''$ and $+10''$. In the case of MB3367, the source is very faint in J and H bands and the blue contours show the position of another star in the slit. Dashed orange lines show the tabulated and observed wavelengths of the lines. Dotted orange lines show the extend of the resolution width. See text for details.

results from Wachter et al. (2010), Gvaramadze et al. (2010), Mauerhan et al. (2011), Wachter et al. (2011), Flagey et al. (2011), Nowak et al. (in prep), and the present paper, the number of identified MBs has more

than doubled, with a total of 128 objects have at least suggested classifications. The fraction of massive evolved stars (candidates) is about half of the “identified” MBs. Table 5 summarizes the statistics of those findings.

Nature	Number	Comments
GK (super)giants	7	
F/G	1	
B/A	2	
B stars	5	from B0 to B9
Be, B[e], and/or LBV	30	Only few are known, <i>bona fide</i> LBV
OB	5	
Oe/WN	2	
WR	13	11 WN, 1 WC or [WC], 1 [WO]
Galaxies	2	
PNe	58	Most central sources not characterized
SNR	3	
Unknown	300	

Table 5

Summary of the identifications of MBs in Mizuno et al. (2010).

Among the 62 shells selected by Wachter et al. (2010), 48 are part of the Mizuno et al. (2010) catalog and all except seven central sources have now been identified. Gvaramadze et al. (2010) established a list of 115 nebulae from their analysis of the first part of the MIPS GAL survey (i.e. $10^\circ < |l| < 65^\circ$) and the Cygnus-X survey. There are 60 MBs in their catalog, 29 of which were not already in the list of Wachter et al. (2010). Among these 29 MBs, 16 remain to be identified. Mauerhan et al. (2011) found a WN8-9h star at the center of one MB, which was also part of the sample of four MBs observed with the high-resolution module of *Spitzer*/IRS by Flagey et al. (2011). Stringfellow et al. (2012a) independently confirmed this star as a WN7-9h. While most of the new identifications have been obtained from optical and near-IR spectra of the central sources, some have also been suggested based on mid-IR spectroscopic observations with *Spitzer*/IRS of the shells, and their central sources when present (Flagey et al. 2011; Nowak et al. in prep). Those unique datasets have revealed a population of highly excited, dust-poor PNe, at the centers of which some types of extreme white dwarf may be hidden, accounting for 9 out of the 14 MBs in this sample. The mid-IR observations have also made possible the characterization of the dust properties in the nebula of 5 dust-rich MBs. These last two studies, although based upon a small number of MBs, indicate that the dust-rich spectra are associated with massive star candidates (e.g. LBV, WR) that are detected in the mid-IR, while the highly excited, dust-poor MBs show no central source in this wavelength range.

Among the 128 “known” MBs, the PN candidates now constitute less than 45%. Most of these have central sources that have not been characterized. Their true natures could thus be different. For instance, MGE333.9202-00.8910 was originally associated with a PN in Mizuno et al. (2010) but Wachter et al. (2011) identified the central source as a B[e]/LBV candidate. The group of Be/B[e]/LBV accounts for almost half of the remaining “known” objects (30/70). Only a few *bona fide* LBV, or LBV candidates suggested by other means, are among this group, including V 481 Sct (MB3280), and Wray 17-96 (MB4562). The ambiguity between the Be, B[e], and LBV phenomena is inherent to near-IR spectroscopic observations of these sources, and only further observations will help us distinguish between the three types (see section 3.3.2). As only a few *bona fide* LBV are known (Clark et al. 2005), and as they are

among the most massive, bright, and extreme stars in terms of mass loss events, the finding of several tens of new candidates could be a major step towards a better understanding of this critical step in the evolution of massive stars toward the WR and SN phases (see e.g. Groh et al. 2013).

The identifications of the central sources in the MBs have also revealed 10 newly discovered WR stars, in addition to the WN5b found via *J*, *K* and narrowband imaging surveys of the Galactic plane (MB4107, Shara et al. 2009). A low-mass [WO 3]pec star (at the center of MB4344, Weidmann et al. 2008) was also known before the publication of the Mizuno et al. (2010) catalog, and a possible [WC5-6] is identified in the present paper. A close pair of WN8-9h (MB3312, MB3313), located at about 5 kpc from the Sun, is among the most striking discoveries, as both mid-IR shells seem to be interacting (Mauerhan et al. 2010; Gvaramadze et al. 2010; Wachter et al. 2010; Burgemeister et al. 2013) and offers an unprecedented view of interacting winds, outflows, and radiations of evolved massive stars. The search for Galactic WR stars has been very active in the recent years as models predict there are ten times as many as are known. The finding here of 10 new Population I WR stars is not a significant contribution to this search, and the detection rate is not competitive with other methods (Mauerhan et al. 2011; Shara et al. 2009, 2012; Faherty et al. 2014; Kanarek et al. 2014). However, the use of the mid-IR as a selection criteria, via the detection of the nebula, could facilitate the discovery of the WR stars hidden by the interstellar extinction in the Galactic plane at shorter wavelengths.

Massive star candidates dominate the new discoveries, i.e. after the publication of the Gvaramadze et al. (2010), Wachter et al. (2010), and Mizuno et al. (2010) catalogs. This is because evolved massive stars are more likely to be surrounded by hot or warm dust, which increases their near- to mid-IR luminosities, while hot, low luminosity white dwarfs remain hidden, especially behind the significant interstellar extinction of the Galactic plane. The sample presented in this paper corresponds to average magnitudes of 11.5, 12.6, and 14.2 in *K*, *H* and *J* bands, respectively. At these magnitudes, and even more at deeper levels, confusion between multiple potential central sources is an issue. Although the UKIDSS survey goes a few magnitudes deeper than 2MASS (*K*~18 mag, Lawrence et al. 2007), about one-third of the MBs still have no clear candidate central sources. On the other

hand, about one-third of the MBs has at least two sources within $2''$ of their geometric center. It will be necessary to use different observational methods to determine the true natures of the remaining ~ 300 unknown MBs. Because of the significant extinction within the Galactic plane, these observations will surely be limited to the IR wavelength range. Near-IR integral field instrument, such as SINFONI on the VLT or NIFS on Gemini-North, would allow one to obtain the spectra of multiple candidate central sources simultaneously.

5. CONCLUSION

We have presented near-IR spectroscopic observations of the central source in 14 circumstellar shells, previously discovered in the *Spitzer*/MIPSGAL 24 μm images of the Galactic plane survey, as well as 3 comparison sources. The near-IR TripleSpec data allowed us to identify:

- 5 late type giants, thanks to the detection of the CO band-head absorption features. We used the equivalent width of the 2.29 μm feature to derive two possible spectral types (one for each of the giant and supergiant class) and ruled out the supergiant interpretation using the inferred distance and total extinction along the line of sight.
- 3 early type stars (B and A), likely supergiants or giants, identified by the strengths and widths of the H and He absorption features. In particular, we revoked the identification of BD+43 3710 as a carbon star, and suggested its spectral class is B5 I, while the true carbon star is the nearby ($\sim 4'$) V2040 Cyg. We used their magnitudes and colors to set constraints on their distances and the sizes of the mid-IR nebulae.
- 4 O and WR stars, characterized by the He II line at 2.1885 μm . We used diagnostics based on line equivalent width ratios and spectral libraries to infer the spectral types of two MBs to be WC5-6, possibly of low mass, and a candidate O5-6, possibly dwarf. The [WC5-6] is a confirmation and refinement of the suggested identification by (Gvaramadze et al. 2010). The two other WR stars are among the three comparison sources. Their spectral types (WN9h and a WN5sh) are in excellent agreement with those derived from optical observations. The three WR stars also exhibit typical broad lines with terminal velocities of 650 and 1700 km/s for the WN9h and WN5sh respectively, and a FWHM of about 1250 km/s for the WC5-6.
- 5 LBV candidates whose near-IR spectra are similar to that of Be or B[e] stars, as shown in several other studies. We followed the notation of Wachter et al. (2010) and labelled them Be/B[e]/LBV. For two of these objects we estimated terminal velocities of 200 and 550 km/s for their stellar winds. For three of these LBV candidates, we confirm their status previously suggested by Wachter et al. (2011) and Stringfellow et al. (2012a).

The long-slit Palomar/TripleSpec observations have also revealed at least two shells in emission in several

H and He lines. The regions traced by the extended line emission have spatial extents in very good agreement with those seen in the mid-IR images. The spreads in velocity of the shells are $\lesssim 150$ km/s. Constraints on the distances to the MBs will allow us to derive, in a future paper, the dust masses in the nebulae, for those that are detected in the Herschel far-IR bands (Flagey & Noriega-Crespo in prep).

Near-IR and optical long-slit spectroscopic observations have now doubled the number of MBs for which natures have been identified or suggested. They have revealed many WR stars and LBV candidates, reducing the fraction of PNe from about 80% when the catalog of Mizuno et al. (2010) was published, to less than 50%. However, the new identifications suffer from selection effects, as these central sources are the brightest of the 428 MBs in the near- to mid-IR, with typical K magnitudes of about 10.5. Because most of the remaining 300 unidentified MBs are within 1° of the Galactic plane and toward the inner Galaxy (63% are within $|l| < 10^\circ$), confusion and extinction are limiting factors that will require the use of near-IR integral field units (e.g. SINFONI on VLT, NIFS on Gemini-North) rather than slit spectrographs to identify the natures of the potential central sources. Deep imaging will also be necessary to find the central sources in the MBs where none are detected so far. The characterization of the mid-IR extended emission of the MBs, which started on a limited sample at the end of *Spitzer*'s cryo-mission, has set constraints on the dust masses and mass loss rates in dust-rich MBs, and revealed peculiar, highly excited, dust-poor objects that may harbor extreme white dwarfs (Flagey et al. 2011; Nowak et al. in prep). Additional such observations will have to wait for the next space mission with mid-IR spectroscopic capabilities: the James Webb Space Telescope.

The Hale Telescope at Palomar Observatory is operated as part of a collaborative agreement between the California Institute of Technology, its divisions Caltech Optical Observatories and the Jet Propulsion Laboratory (operated for NASA), and Cornell University. This research has made use of the SIMBAD database, operated at CDS, Strasbourg, France, and of the NASA/IPAC Infrared Science Archive, which is operated by the Jet Propulsion Laboratory, California Institute of Technology, under contract with the National Aeronautics and Space Administration. NF thanks Francois Ochsenbein for providing the plate scale of the BD charts, Paul Crowther for his help with some identifications, and the referee for very valuable comments. TRGs research is supported by the Gemini Observatory, which is operated by the Association of Universities for Research in Astronomy, Inc., on behalf of the international Gemini partnership of Argentina, Australia, Brazil, Canada, Chile, and the United States of America.

REFERENCES

- Aaronson, M., Blanco, V. M., Cook, K. H., Olszewski, E. W., & Schechter, P. L. 1990, ApJS, 73, 841
 Allen, C. 1983, Astrophysical Quantities (London: Athlone Press)
 Barniske, A., Oskina, L. M., & Hamann, W.-R. 2008, A&A, 486, 971
 Benjamin, R. A., Churchwell, E., Babler, B. L., et al. 2003, PASP, 115, 953

- Bjorkman, K. S., Miroshnichenko, A. S., Bjorkman, J. E., et al. 1998, *ApJ*, 509, 904
- Burgemeister, S., Gvaramadze, V. V., Stringfellow, G. S., et al. 2013, *MNRAS*, 429, 3305
- Cardelli, J. A., Clayton, G. C., & Mathis, J. S. 1989, *ApJ*, 345, 245
- Carey, S. J., Noriega-Crespo, A., Mizuno, D. R., et al. 2009, *PASP*, 121, 76
- Clark, J. S., Larionov, V. M., & Arkharov, A. 2005, *A&A*, 435, 239
- Collins, II, G. W. 1987, in *IAU Colloq. 92: Physics of Be Stars*, ed. A. Slettebak & T. P. Snow, 3–19
- Cox, A. N. 2000, *Allen's astrophysical quantities*
- Crowther, P. A. 2007, *ARA&A*, 45, 177
- Crowther, P. A., Hadfield, L. J., Clark, J. S., Negueruela, I., & Vacca, W. D. 2006, *MNRAS*, 372, 1407
- Cushing, M. C., Vacca, W. D., & Rayner, J. T. 2004, *PASP*, 116, 362
- Davies, B., Figer, D. F., Kudritzki, R.-P., et al. 2007, *ApJ*, 671, 781
- Egilitis, I., Eglite, M., & Balklavs, A. 2003, *Baltic Astronomy*, 12, 353
- Faherty, J. K., Shara, M. M., Zurek, D., Kanarek, G., & Moffat, A. F. J. 2014, *AJ*, 147, 115
- Figer, D. F., MacKenty, J. W., Robberto, M., et al. 2006, *ApJ*, 643, 1166
- Figer, D. F., McLean, I. S., & Najarro, F. 1997, *ApJ*, 486, 420
- Flagey, N. & Noriega-Crespo, A. in prep
- Flagey, N., Noriega-Crespo, A., Billot, N., & Carey, S. J. 2011, *ApJ*, 741, 4
- Furness, J. P., Crowther, P. A., Morris, P. W., et al. 2010, *MNRAS*, 403, 1433
- Groh, J. H., Meynet, G., & Ekström, S. 2013, *A&A*, 550, L7
- Gvaramadze, V. V., Fabrika, S., Hamann, W.-R., et al. 2009, *MNRAS*, 400, 524
- Gvaramadze, V. V., Kniazev, A. Y., & Fabrika, S. 2010, *MNRAS*, 405, 1047
- Gvaramadze, V. V. & Menten, K. M. 2012, *A&A*, 541, A7
- Gvaramadze, V. V., Weidner, C., Kroupa, P., & Pflamm-Altenburg, J. 2012, *MNRAS*, 424, 3037
- Hamann, W.-R., Gräfener, G., & Liermann, A. 2006, *A&A*, 457, 1015
- Hanson, M. M., Kudritzki, R.-P., Kenworthy, M. A., Puls, J., & Tokunaga, A. T. 2005, *ApJS*, 161, 154
- Humphreys, R. M. & Davidson, K. 1994, *PASP*, 106, 1025
- Ingallinera, A., Triglio, C., Umana, G., et al. 2014, *MNRAS*, 437, 3626
- Jaschek, M., Slettebak, A., & Jaschek, C. 1981, *Be star terminology*, *be Star Newsletter*
- Kanarek, G. C., Shara, M. M., Faherty, J. K., Zurek, D., & Moffat, A. F. J. 2014, *ArXiv e-prints*
- Kohoutek, L. 2001, *A&A*, 378, 843
- Kraemer, K. E., Hora, J. L., Egan, M. P., et al. 2010, *AJ*, 139, 2319
- Lamers, H. J. G. L. M., Zickgraf, F., de Winter, D., Houziaux, L., & Zorec, J. 1998, *A&A*, 340, 117
- Lancon, A. & Rocca-Volmerange, B. 1992, *A&AS*, 96, 593
- Lawrence, A., Warren, S. J., Almaini, O., et al. 2007, *MNRAS*, 379, 1599
- Lenorzer, A., de Koter, A., & Waters, L. B. F. M. 2002, *A&A*, 386, L5
- Leuhenagen, U., Hamann, W., & Jeffery, C. S. 1996, *A&A*, 312, 167
- Mauerhan, J. C., Van Dyk, S. D., & Morris, P. W. 2011, *AJ*, 142, 40
- Mauerhan, J. C., Wachter, S., Morris, P. W., Van Dyk, S. D., & Hoard, D. W. 2010, *ApJ*, 724, L78
- Meyer, M. R., Edwards, S., Hinkle, K. H., & Strom, S. E. 1998, *ApJ*, 508, 397
- Miszalski, B., Parker, Q. A., Acker, A., et al. 2008, *MNRAS*, 384, 525
- Mizuno, D. R., Kraemer, K. E., Flagey, N., et al. 2010, *AJ*, 139, 1542
- Morris, P. W., Eenens, P. R. J., Hanson, M. M., Conti, P. S., & Blum, R. D. 1996, *ApJ*, 470, 597
- Nassau, J. J. & Blanco, V. M. 1954, *ApJ*, 120, 129
- Nota, A., Livio, M., Clampin, M., & Schulte-Ladbeck, R. 1995, *ApJ*, 448, 788
- Nowak, M., Flagey, N., Noriega-Crespo, A., Billot, N., & Carey, S. J. in prep
- Parker, Q. A., Acker, A., Frew, D. J., et al. 2006, *MNRAS*, 373, 79
- Parker, Q. A. & Morgan, D. H. 2003, *MNRAS*, 341, 961
- Pickles, A. J. 1998, *PASP*, 110, 863
- Porter, J. M. & Rivinius, T. 2003, *PASP*, 115, 1153
- Rayner, J. T., Cushing, M. C., & Vacca, W. D. 2009, *ApJS*, 185, 289
- Reid, M. J., Menten, K. M., Zheng, X. W., et al. 2009, *ApJ*, 700, 137
- Sander, A., Hamann, W.-R., & Todt, H. 2012, *A&A*, 540, A144
- Shara, M. M., Faherty, J. K., Zurek, D., et al. 2012, *AJ*, 143, 149
- Shara, M. M., Moffat, A. F. J., Gerke, J., et al. 2009, *AJ*, 138, 402
- Skrutskie, M. F., Cutri, R. M., Stiening, R., et al. 2006, *AJ*, 131, 1163
- Stencel, R. E., Pesce, J. E., & Bauer, W. H. 1989, *AJ*, 97, 1120
- Stringfellow, G. S., Gvaramadze, V. V., Beletsky, Y., & Kniazev, A. Y. 2012a, in *IAU Symposium*, Vol. 282, *IAU Symposium*, ed. M. T. Richards & I. Hubeny, 267–268
- Stringfellow, G. S., Gvaramadze, V. V., Beletsky, Y., & Kniazev, A. Y. 2012b, in *Astronomical Society of the Pacific Conference Series*, Vol. 465, *Proceedings of a Scientific Meeting in Honor of Anthony F. J. Moffat*, ed. L. Drissen, C. Rubert, N. St-Louis, & A. F. J. Moffat, 514
- Urquhart, J. S., Hoare, M. G., Purcell, C. R., et al. 2009, *A&A*, 501, 539
- Vacca, W. D., Cushing, M. C., & Rayner, J. T. 2004, *PASP*, 116, 352
- van der Hucht, K. A. 2001, *New Astron. Rev.*, 45, 135
- Voors, R. H. M., Geballe, T. R., Waters, L. B. F. M., Najarro, F., & Lamers, H. J. G. L. M. 2000, *A&A*, 362, 236
- Wachter, S., Mauerhan, J., van Dyk, S., Hoard, D. W., & Morris, P. 2011, *Bulletin de la Societe Royale des Sciences de Liege*, 80, 291
- Wachter, S., Mauerhan, J. C., Van Dyk, S. D., et al. 2010, *AJ*, 139, 2330
- Wallace, L., Meyer, M. R., Hinkle, K., & Edwards, S. 2000, *ApJ*, 535, 325
- Weidmann, W. A., Gamen, R., Díaz, R. J., & Niemela, V. S. 2008, *A&A*, 488, 245
- Whittet, D. C. B., ed. 2003, *Dust in the galactic environment*
- Young, K., Phillips, T. G., & Knapp, G. R. 1993, *ApJ*, 409, 725